Original Article

Spatial Optimization and District-Level Allocation of Heat-Health Relief Centers in West Bengal, India: A Location-Allocation Modeling Study

Shuvajit Roy[1]. Anurag Mondal[2]

[1]Senior Resident, Department of Community Medicine, Sarat Chandra Chattopadhyay Government Medical College & Hospital, Uluberia

[2]Senior Resident, Department of Community and Family Medicine, All India Institute of Medical Sciences, Guwahati, Assam, India

Abstract

Background: The increasing frequency and intensity of extreme thermal events pose a severe public health hazard across West Bengal. Conventional ad-hoc infrastructure planning routinely favors ultra-dense metropolitan centers, leaving marginalized peripheral communities critically unprotected. The aim of this study deployed a prescriptive Capitated p-Median location-allocation optimization routine using a multi-dimensional Heat-Health Vulnerability Index (HHVI) to mathematically anchor 20 district-level emergency cooling centers across 840 community clusters. This study deployed a prescriptive Capitated p-Median location-allocation optimization routine using a multi-dimensional Heat-Health Vulnerability Index (HHVI) to mathematically anchor 20 district-level emergency cooling centers across 840 community clusters. **Material and Methods:** Regional distances were modeled using the Haversine Great-Circle Distance formula. Statistical analysis used: To balance operational efficiency with regional administrative equity, a spatially stratified policy scenario was executed to secure exactly one relief medoid within each individual district boundary. **Results:** The empirical HHVI revealed an extensive continuous risk gradient spanning from 0.0873 to 0.6293. Built-environment insulation traps (Iroof) held the strongest positive correlation with vulnerability (r = 0.6956). Conversely, population density displayed a notable negative correlation (r = -0.3143), revealing an "urban infrastructure paradox" where dense metropolitan centers enjoy superior structural adaptive capacity over isolated rural areas. The optimization algorithm successfully selected urban locations in 15 districts but dynamically bypassed metropolitan bias to establish rural hubs in five agricultural zones, where severe housing deficits and absolute medical isolation overrode raw population density. **Conclusion:** This spatial optimization framework provides disaster management authorities with a scientifically validated blueprint to maximize climate resilience and equitable public health protection.

Keywords: Climate Change, Cooling Centers, Heat Stress, India, Spatial Analysis, Vulnerable Population.

Received: 17 April 2026 **Revised: 04 May 2026** **Accepted: 26 May 2026** **Published: 06 June 2026**

Introduction

The accelerating pace of global climate change, driven primarily by anthropogenic greenhouse gas emissions, has fundamentally transformed the global thermodynamic equilibrium, leading to an unprecedented rise in global mean surface temperatures.[1] Among the multi-sectoral consequences of global warming, the amplification of extreme weather events, specifically the increased frequency, intensity, and duration of heatwaves, presents an immediate and existential threat to human survivability and public health systems worldwide.[2] The Intergovernmental Panel on Climate Change (IPCC) has consistently warned that under unmitigated emission scenarios, hot extremes that occurred once every 50 years in the pre-industrial era will happen roughly 40 times more frequently, fundamentally shifting ambient environmental conditions from seasonal anomalies to chronic occupational and environmental hazards.[3]

This global thermal paradigm translates directly into localized human biometeorological stress. Heat stress manifests when the human body's core thermoregulatory mechanisms are overwhelmed by a combination of high ambient dry-bulb temperature, elevated relative humidity, low wind speed, and intense solar radiation.[4] When the environmental heat load exceeds the physiological capacity for metabolic heat dissipation—primarily achieved via the evaporation of sweat, individuals experience rapid elevations in core body temperature, leading to severe clinical outcomes including heat exhaustion, heat syncope, and fatal heat stroke.[5] Human vulnerability to these thermal anomalies, however, is not uniform; it is a complex, latent construct shaped by the intersection of absolute environmental exposure, intrinsic demographic sensitivity, and structural adaptive capacity.[6]

In the regional context of South Asia, the sub-tropical and tropical landscapes of West Bengal, India, have emerged as highly critical theaters of escalating thermal distress.[7] Over the past few decades, meteorological trend analyses across West Bengal have recorded a significant upward shift in both maximum and minimum baseline temperatures, alongside an

Address for correspondence: Dr. Anurag Mondal, Senior Resident, Department of Community and Family Medicine, All India Institute of Medical Sciences, Guwahati, Assam, India.
E-mail: shuva6850@gmail.com

DOI:
10.21276/amit.2026.v13.i2.713

How to cite this article: Roy S. Mondal A. Spatial Optimization and District-Level Allocation of Heat-Health Relief Centers in West Bengal, India: A Location-Allocation Modeling Study. Acta Med Int. 2026;13(2):402-410.

alarming extension of the pre-monsoon heatwave window deep into the Gangetic plains and the western undulating terrains.[8] Urban agglomerations, such as the Kolkata metropolitan area, suffer from intense urban heat island (UHI) effects, trapping nocturnal thermal radiation due to dense concrete infrastructure and low albedo surfaces.[9] Concurrently, the rural and coastal districts experience compounding heat hazards, where high ambient air temperatures interact with intense maritime relative humidity from the Bay of Bengal, producing extreme Heat Index readings that compromise human physiological cooling efficiency for extended periods.[10]

Within this escalating hazard landscape, specific sub-populations bear a disproportionate burden of health risks. From an epidemiological and demographic perspective, the elderly (aged over 60 years) and children under five years represent highly sensitive cohorts due to compromised or underdeveloped autonomic thermoregulatory responses.[11] Furthermore, socio-economic marginalization heavily determines adaptive capacity. Low-income families residing in informal settlements or rural areas are routinely confined within structurally vulnerable housing—characterized by thermally conductive tin, asbestos, or corrugated iron roofing sheets—which creates severe indoor microclimatic heat traps.[12] These exposures are further worsened by widespread lack of domestic cooling infrastructure, lack of continuous electricity, and significant physical isolation from tertiary healthcare networks, placing outdoor manual laborers, rural agricultural workers, and marginalized socio-demographic communities at the frontline of heat-induced morbidity and mortality.[13]

To mitigate this acute public health crisis, deploying emergency cooling centers represents a vital, novel structural intervention within municipal and rural heat action plans.[14] Designed as air-conditioned, geophysically accessible public sanctuaries, these emergency centers provide immediate physiological relief, active hydration support, and essential medical triaging during peak thermal hours, effectively breaking the continuous accumulation of internal heat stress in highly vulnerable individuals.[15] However, the physical deployment of these life-saving facilities faces severe regional logistical constraints. In a socio-economically and geographically diverse state like West Bengal, establishing fully equipped cooling hubs across every single administrative sub-division or local block is operationally unfeasible due to baseline deficits in specialized grid power, medical staffing, and real-time administrative oversight.[16] Consequently, public health planning dictates a spatially stratified phased implementation strategy, mandating the establishment of exactly one mathematically optimized emergency relief hub anchored within the boundaries of each individual district.[17]

Given these logistical parameters, the allocation of emergency infrastructure cannot rely on ad-hoc or purely politically driven administrative decisions. Assuming that sufficient fiscal budget has been allocated by state disaster management authorities to establish these regional facilities, the core public health challenge shifts to a problem of spatial optimization: identifying the exact geographic coordinates within each district that maximize public health outcomes.[18] Selecting these sites requires an advanced spatial optimization framework that integrates multi-sectoral datasets, incorporating microclimatic baseline hazards, demographic density markers, built-environment vulnerabilities, and physical distances to existing hospital networks.[19]

Therefore, the primary objective of this study is to implement a Capitated p-Median location-allocation optimization routine using a localized Heat-Health Vulnerability Index (HHVI) as the demand weight matrix. By resolving the spatial impedance between vulnerable populations and emergency infrastructure across 840 clusters, this research aims to provide a definitive, scientifically validated blueprint for the strategic placement of 20 district-level cooling centers, ensuring equitable, maximum-impact public health protection against the compounding realities of climate change in West Bengal.

Materials and Methods

Study Area and Study Unit: This secondary data analysis was conducted across the state of West Bengal, India, situated between 21°25'N to 27°13'N latitude and 85°50'E to 89°50'E longitude. The state features diverse microclimates, ranging from the humid, tropical Gangetic plains and coastal Sundarbans delta in the south to the arid, drought-prone plateau regions in the west, and alpine terrain in the north. The primary spatial unit of analysis comprises 840 georeferenced community clusters derived from the National Family Health Survey (NFHS-5) framework. This multi-district administrative network spans 20 distinct districts, creating substantial environmental, socio-demographic, and infrastructural gradients that govern localized vulnerability profiles.

Study Variables and Data Sources: To construct a robust multi-dimensional framework for climate risk, the following variables were compiled and spatially linked from multiple government records, open-access crowdsourced platforms, and remote sensing cloud registries:

Socio-Demographic Sensitivity: Baseline human exposure parameters, including population density (people per square kilometer), localized illiteracy rates (%), and the population proportion belonging to historically marginalized groups (Scheduled Castes and Scheduled Tribes, %), were collected from the Primary Census Abstract and District Wards Directory series published by the Office of the Registrar General & Census Commissioner, Ministry of Home Affairs, Government of India.[20]

Granular household indicators, specifically the concentration of highly sensitive age groups (proportions of children under 5 years and elderly over 60 years of age) and gender-based vulnerability indicators (proportions of female-headed households), were extracted from the microdata files of the National Family Health Survey (NFHS-5) distributed via the DHS Program Spatial Data Repository.[21]

Physical Surface Exposure: Environmental indicators were extracted via automated spatial pixel-reduction scripts executed across imagery collection archives within the Google Earth Engine (GEE) platform [22]. Variations in canopy cover and surface greenness were captured using the Normalized Difference Vegetation Index (NDVI) derived from Landsat 8/9

multi-spectral surface reflectance bands. Artificial sealing and concrete footprints were modeled via the European Commission's Global Human Settlement Layer (GHSL) built-up density grids. Land Surface Temperature (LST) configurations were derived from daily thermal infrared bands of the NASA MODIS satellite platform (MOD11A1/MYD11A1).

Adaptive Capacity & Infrastructure Gaps: Building-scale vulnerability indicators, such as the proportion of households constructed with highly conductive roofing sheets (tin or asbestos) and the percentage of dwellings facing a severe utility deficit (lacking concurrent access to domestic electricity and municipal water), were obtained from the household questionnaire modules of the survey clusters. Area-level economic buffer capacity was mapped using Net District Domestic Product (NDDP) per capita values published in the District Statistical Handbook series by the Bureau of Applied Economics and Statistics, Government of West Bengal.[23] Geographic physical isolation from emergency medical systems was modeled as the absolute shortest distance (in kilometers) to the nearest secondary or tertiary care healthcare hub, generated from point vectors matching registered medical amenities from the OpenStreetMap database via the Overpass API, cross-verified with the ISRO Bhuvan Indian Geo-Platform.[24]

Heat Index Calculation: Maximum ambient dry-bulb air temperature and relative humidity were acquired as gridded daily datasets from the Indian Meteorological Department (IMD) data supply portal and supplemented via the NASA POWER database.[25] Because dry ambient temperature alone underestimates human physiological heat stress under humid tropical conditions, the atmospheric baseline hazard was modeled using the Heat Index (HI). Also known as apparent temperature, the Heat Index quantifies the bioclimatic stress perceived by the human body by mathematically combining air temperature and relative humidity. This relationship models the severe reduction in human evaporative cooling efficiency caused by high moisture content in the air.

The baseline Heat Index for each spatial cluster was derived by solving the multi-variable regression equation developed by the United States National Weather Service (NWS), which refines Robert G. Steadman's mathematical biometeorological model.[26,27]

Data Extraction and Normalization: To prevent scale-dependent mathematical bias during index aggregation, a linear transformation was applied to standardize all indicators onto a unitless, continuous gradient bounded strictly between 0 (representing maximum resilience or minimum baseline hazard) and 1 (representing maximum structural exposure or systemic deprivation). This was executed via linear Min-Max normalization,[28]

$$I_{k,i} = \frac{X_{k,i} - min\,(X_k)}{max\,(X_k) - min\,(X_k)}$$

Where:

- Ik,i represents the normalized, standardized value for indicator k at spatial survey cluster i.
- Xk,i denotes the raw empirical value observed for that cluster.
- min (Xk) and max (Xk) represent the absolute minimum and maximum values observed for variable k across the global 840-cluster matrix.

2.6. HHVI Formulation: Following individual variable standardization, five core indicator domains were selected from the processed database to represent compounding axes of exposure, sensitivity, and adaptive deprivation. These sub-indices were aggregated using an unweighted arithmetic mean to compile the latent Heat-Health Vulnerability Index (HHVI) for each cluster i:

$$HHVI_i = \frac{I_{heat,i} + I_{density,i} + I_{sensitive,i} + I_{roof,i} + I_{distance,i}}{5}$$

Where the structural sub-indices are operationally defined as:

- $\mathbf{I_{heat,i}}$**:** The standardized Thermal Exposure Index, derived from the calculated atmospheric Heat Index.
- $\mathbf{I_{densityt,i}}$**:** The standardized Crowding Exposure Index, derived from population density per square kilometer.
- $\mathbf{I_{sensitive,i}}$**:** The standardized Demographic Sensitivity Index, representing the combined population percentage of pediatric (age < 5) and geriatric (age > 60) cohorts.
- $\mathbf{I_{roof,i}}$**:** The standardized Built-Environment Trap Index, representing the percentage of households structurally limited by conductive tin or asbestos roofing sheets.
- $\mathbf{I_{distance,i}}$**:** The standardized Baseline Healthcare Deprivation Index, quantifying geographic isolation via physical distance to the nearest emergency medical facility.

The resulting $\mathbf{HHVI_i}$ provides a continuous gradient bounded within [0, 1], where values approaching unity designate acute socio-ecological vulnerability hotspots.

2.7. Demand Weight and Great Circle Projection: While the **HHVI** standardizes individual vulnerability, it does not inherently account for the absolute volume of human life exposed within a given spatial container. To transform this descriptive index into an operational resource-allocation metric, a localized Demand Weight ($\mathbf{W_i}$) was formulated for each cluster. This parameter acts as the continuous volume of risk demanding emergency response interventions, derived by scaling the latent HHVI against the baseline population density:

$$W_i = HHVI_i\ x\ (Population\ Density_i + 1)$$

A constant offset of 1 was introduced to the baseline population density to preserve the underlying environmental and structural hazard scores in sparsely populated rural zones, preventing the complete mathematical nullification of demand weights in low-density geographies.

Because flat-plane Euclidean spatial models introduce significant geometric distortion over state-level regional expanses, regional distances were modeled along the true ellipsoidal curvature of the Earth. For every spatial cluster pair (**i, j**) in the set of all clusters **N (|N| = 840)**, the absolute shortest geographical distance ($\mathbf{D_{ij}}$) was computed using the Haversine Great-Circle Distance formula [29]:

$$D_{ij} = 2R\,.\,arcsin\left(\sqrt{sin^2\left(\frac{\Delta\phi_{ij}}{2}\right) + cos(\phi_i)\,cos\,(\phi_j)\,sin^2\left(\frac{\Delta\lambda_{ij}}{2}\right)}\right)$$

Where R represents the mean radius of the Earth (~6371 km), ϕ_i and ϕ_j denote the geodetic latitudes of clusters **i** and **j** expressed

in radians, $\Delta\phi_{ij} = \phi_i - \phi_j$ represents the latitudinal delta, and $\Delta\lambda_{ij} = \lambda_i - \lambda_j$ represents the longitudinal delta between the coordinates of the two locations. A complete, symmetric geographic impedance matrix of dimension 840 × 840 was pre-computed to govern the spatial interaction constraints of the optimization model.

2.8. Spatial Optimization and Policy Scenario Formulation

To transition from passive vulnerability mapping to active structural mitigation, a Capitated **p**-Median Location-Allocation Model was deployed [30]. The objective of this framework is prescriptive: select a set of optimal facility locations (such as emergency cooling stations or specialized mobile clinics) out of the pool of 840 candidate clusters to maximize geographical accessibility and minimize the collective public health burden. To bridge the gap between absolute operational efficiency and administrative equity, the optimization problem was modeled under two distinct policy scenarios:

Scenario A: Global Centralized Optimization (Administrative Efficiency)

Scenario A frames resource allocation through a lens of maximum state-wide efficiency, evaluating all 840 clusters simultaneously regardless of their containing borders. The mathematical optimization problem is framed to minimize the aggregate, vulnerability-weighted travel distance across the entire population network:

$$\min \sum_{i \in N} W_i \min_{j \in S} D_{ij}$$

Subject to the structural constraints:

$$S \subset N, |S| \; p_{global}$$

Where **N** represents the global set of all clusters **(**|**N**|=840), **S** represents the localized subset of selected facility nodes, and p_{global} denotes the total facility allocation budget, fixed at **p** = 6 for this scenario. The term $\min_{j \in S} D_{ij}$ enforces a strict closest-facility assignment rule, meaning every vulnerable cluster **i** is automatically served by its geographically closest emergency center **j**.

Scenario B: Spatially Stratified Optimization (Regional Administrative Equity)

Scenario B aligns the prescriptive model with decentralized public health governance and ensures geographical equity across administrative boundaries. Rather than pooling all clusters into a single state-wide competition, which inherently skews resource allocation toward ultra-dense metropolitan cores, this policy scenario mandates the strategic establishment of exactly one (p_d = 1) optimal heat relief node within the borders of every individual district in West Bengal.

Let **D** represent the complete set of administrative districts, where each district **d** contains a mutually exclusive subset of survey clusters N_d (such that the union of all subsets equals **N**). The mathematical objective function shifts from a global minimization to a series of localized, independent optimization layers. For each discrete district, the algorithm identifies a singular facility anchor (**j***) that minimizes the localized, vulnerability-weighted travel distance network: For each district d

$$d \in D, \quad \min \sum_{i \in N_d} W_i \min_{i \in N_d} D_{i,i^*}$$

Subject to the strict intra-district assignment constraint:

$j^* \in N_d$

This operational shift ensures that regional microclimates, unique local built-environment vulnerabilities, and structural healthcare isolation factors are evaluated relative to their immediate peer clusters within the same district boundary, providing actionable, highly tailored blueprints for local district health authorities.

2.9. Algorithmic Execution and Computational Architecture

Due to the combinatorial complexity of evaluating facility configurations within an 840 × 840 spatial solution space, an iterative Greedy Forward Selection Heuristic was operationalized to find the global cost minima under Scenario A, while a direct medoid search was completed for Scenario B [31].

Algorithm 1: Greedy Forward Selection for the Global p-Median Problem (Scenario A)

Input: Set of all clusters N, Distance Matrix D, Demand Weights W, Target facility allocation number p_global

Output: Optimized subset of facilities S

1. Initialize S ← ∅
2. for step k = 1 to p_global do
3. best_cost ← ∞
4. best_candidate ← -1
5. for each candidate j ∈ N \ S do
6. Test_Set ← S ∪ {j}
7. Current_Cost ← ∑_{i ∈ N} (W_i × min_{m ∈ Test_Set} D_im)
8. if Current_Cost < best_cost then
9. best_cost ← Current_Cost
10. best_candidate ← j
11. end if
12. end for
13. S ← S ∪ {best_candidate} // Permanently lock the optimal node
14. end for
15. return S

Before running the optimization scripts, a data-cleansing sweep was executed to handle spatial anomalies. Geometric coordinate anomalies, specifically a surveyed urban cluster in the Hugli district, display missing or null coordinates at 0.0°N, 0.0°E, and were systematically corrected by calculating the localized spatial mean derived from neighboring urban cluster coordinates within that specific district sub-population, yielding an imputed position of 22.786866°N, 88.285360°E. All normalization pipelines, distance matrix calculations, and greedy interchange optimization loops were executed using the Python programming environment (v3.10), utilizing the pandas, geopandas, and scipy. spatial numerical computation libraries. Spatial layouts, vulnerability gradients, and final site allocations were mapped using matplotlib and seaborn visualization engines.

2.10. District-Wise Location: To guarantee empirical validity, the exact mathematical constraints calculated by the Python runtime for the decentralized regional equity model (Scenario B) are locked into the model parameters.

2.11. Ethical Considerations: This study is based on de-identified secondary data available on public domains, it does not require any ethical permission. However, all the terms and conditions stated by competent authorities were maintained

throughout the work.

Results

3.1. Spatial Gradients and Composite Profiles of Heat-Health Vulnerability: The empirical calculation of the Heat-Health Vulnerability Index (**HHVI**) across the 840 spatial clusters in West Bengal revealed an extensive continuous risk gradient, with scores spanning from an absolute resilient baseline of 0.0873 to a maximum acute hotspot value of 0.6293. The state-wide mean vulnerability index settled at 0.3705 ± 0.0755, illustrating a highly diversified landscape of climate vulnerability. A total of 101 spatial clusters exhibited critical vulnerability profiles exceeding an **HHVI** threshold of 0.45, while 19 hyper-acute hotspots crossed the extreme 0.50 margin. When aggregated at the district level, the analysis revealed that the highest mean vulnerability scores were concentrated in the marginalized rural-agricultural and arid western belts, led by Uttar Dinajpur (Mean **HHVI** = 0.4222), Paschim Medinipur (Mean **HHVI** = 0.4215), Purulia (Mean **HHVI** = 0.4210), Bankura (Mean **HHVI** = 0.4159), and Dakshin Dinajpur (Mean **HHVI** = 0.4136). Conversely, the lowest regional vulnerability averages were observed in the highly industrialized sub-region of Paschim Barddhaman (Mean **HHVI** = 0.3027) and the northern alpine ecosystems of Darjeeling (Mean **HHVI** = 0.1814), proving that socio-ecological context heavily mediates how climate stress manifests geographically. (Table 1)

3.2. Empirical Drivers and Indicator Correlation Analysis: To identify the structural dimensions governing heat vulnerability, a Pearson correlation matrix was calculated between the composite **HHVI** and its individual normalized sub-indices. The results demonstrated that the built-environment infrastructure trap, mapped via the presence of highly conductive roofing materials ($\mathbf{I_{roof}}$), maintained the strongest positive relationship with overall vulnerability (**r** = 0.6956, **p** < 0.001$), emphasizing that poor residential thermal insulation acts as a core driver of domestic heat stress. Baseline healthcare deprivation, measured as physical distance to emergency clinical infrastructure ($\mathbf{I_{distance}}$), also demonstrated a prominent positive correlation (**r** = 0.5564, **p** < 0.001$), followed closely by the baseline microclimatic hazard index ($\mathbf{I_{heat}}$, **r** = 0.4563) and demographic age sensitivity ($\mathbf{I_{sensitive}}$, **r** = 0.3896$). Crucially, population density ($\mathbf{I_{density}}$) displayed a notable negative correlation with the overall index (**r** = -0.3143, **p** < 0.001). This negative coefficient uncovers a critical "urban infrastructure paradox": while hyper-dense metropolitan cores like Kolkata and Howrah suffer from extreme raw microclimatic exposure, their highly concentrated medical networks, universal electricity access, and modern built environments significantly lower their structural vulnerability. In contrast, geographically isolated, lower-density rural clusters are frequently penalized by the compounding effects of poor housing stock and systemic healthcare deficits, lifting their composite **HHVI** scores.

3.3. Microclimatic Heterogeneity and Bioclimatic Human Stress: The atmospheric baseline hazard, captured through the calculated U.S. National Weather Service Heat Index (HI), confirmed that looking at ambient air temperature alone systematically underestimates human physiological heat strain in humid tropical zones. The microclimatic data varied from an alpine minimum of 55.81°C in the urban heights of Darjeeling (Cluster 32710) to an extreme baseline of 139.16°C in the industrial corridors of Hooghly (Cluster 33823), reflecting how localized relative humidity multiplies thermal hazards. In the southern deltaic and coastal regions, the atmospheric interaction of elevated ambient temperatures with intense humidity levels produced critical bioclimatic risk profiles, as highlighted by severe localized Heat Index readings in South 24 Parganas (Cluster 34338 at 134.14°C), Haora (Cluster 34118 at 133.26°C), and Kolkata (Cluster 34238 at 132.27°C). These southern urbanized centers exhibited the highest possible continuous thermal exposure sub-index scores ($\mathbf{I_{heat}}$, ranging from 0.8759 to 0.9483), creating an environment where natural human evaporative cooling mechanisms are severely compromised during peak heat waves.

3.4. Capitated p-Median Optimization and Spatial Allocation Routines: To eliminate urban centering bias and guarantee administrative equity across the state, a capitated **p**-median location-allocation routine was executed to fix exactly one ($\mathbf{p_d}$ = 1) optimal heat relief center within each of the 20 administrative districts. By evaluating the symmetric 840 * 840 Haversine impedance matrix against localized demand weights, the mathematical models anchored precise medoid coordinates for each district's relief hub. In the northern zone, the optimal relief anchors were locked at Cluster 32710 in derailing ($\mathbf{I_{heat}}$ = 0.0726, **HHVI** = 0.1438, Urban), Cluster 32826 in Jalpaiguri ($\mathbf{I_{heat}}$ = 0.5551, **HHVI** = 0.3689, Urban), and Cluster 32901 in Koch Bihar ($\mathbf{I_{heat}}$ = 0.6324, **HHVI** = 0.2690, Urban). Moving into the central and agrarian plains, the models designated Cluster 33032 in Uttar Dinajpur ($\mathbf{I_{heat}}$ = 0.6161, **HHVI** = 0.3671, Rural), Cluster 33120 in Dakshin Dinajpur ($\mathbf{I_{heat}}$ = 0.5893, **HHVI** = 0.2897, Urban), Cluster 33226 in Maldah ($\mathbf{I_{heat}}$ = 0.7714, **HHVI** = 0.3740, Urban), and Cluster 33330 in Murshidabad ($\mathbf{I_{heat}}$ = 0.7375, **HHVI** = 0.4909, Rural). For the western arid and central industrial belts, the geographic anchors were established at Cluster 33436 in Birbhum ($\mathbf{I_{heat}}$ = 0.6518, **HHVI** = 0.2829, Urban), Cluster 33901 in Bankura ($\mathbf{I_{heat}}$ = 0.6092, **HHVI** = 0.3399, Urban), Cluster 34015 in Purulia ($\mathbf{I_{heat}}$ = 0.7020, **HHVI** = 0.3066, Urban), Cluster 93111 in Paschim Barddhaman ($\mathbf{I_{heat}}$ = 0.5872, **HHVI** = 0.2636, Urban), and Cluster 93232 in Purba Barddhaman ($\mathbf{I_{heat}}$ = 0.7450, **HHVI** = 0.4621, Rural).

3.5. Sectoral Distribution and Emergency Resource Accessibility: The final optimization runtime showed a strong preference for urban environments, selecting urban nodes in 15 of the 20 administrative districts. This trend reflects the model's objective function, which scales vulnerability directly against underlying population totals to maximize the absolute volume of human lives shielded within localized areas. This pattern is clear in the highly populated southern core, where centers were placed at Cluster 33625 in Nadia (**HHVI** = 0.3195, Urban), Cluster 33739 in North 24 Parganas (**HHVI** = 0.3370, Urban), Cluster 33823 in Hooghly (**HHVI** = 0.2855, Urban), Cluster 34118 in Howrah (**HHVI** = 0.2204, Urban), Cluster 34238 in Kolkata (**HHVI** = 0.3038, Urban), Cluster 34338 in South 24 Parganas (**HHVI** = 0.4393, Urban), and Cluster 34436 in Paschim

Medinipur (**HHVI** = 0.3481, Urban). However, the optimization framework avoided metropolitan bias in highly agricultural or geographically dispersed settings. In Uttar Dinajpur (Cluster 33032), Murshidabad (Cluster 33330), Purba Medinipur (Cluster 34518; $\mathbf{I_{heat}}$ = 0.8399, **HHVI** = 0.3960, Rural), and Purba Barddhaman (Cluster 93232), the model bypassed local urban points to establish emergency hubs within the rural sector. In these specific districts, severe built-environment risks ($\mathbf{I_{roof}}$ up to 0.8418) combined with extensive healthcare isolation ($\mathbf{I_{distancet}}$ up to 0.4479) mathematically overcame basic urban population counts. This mechanism protected peripheral rural populations, preventing them from being marginalized by resource allocation models driven purely by population density. [Table 1 & Figure 1]

Table 1: The exact, uncoerced clusters selected as the absolute mathematical anchors for each district

District Profile	Optimal Cluster ID	Sector	Model Latitude	Model Longitude	Cluster HHVI	Local Heat Index (°C)
Darjeeling	32710	Urban	26.7221°N	88.4209°E	0.144	55.81
Jalpaiguri	32826	Urban	26.5204°N	89.2080°E	0.369	101.73
Koch Bihar	32901	Urban	26.3213°N	89.4428°E	0.269	109.09
Uttar Dinajpur	33032	Rural	25.7915°N	88.1001°E	0.367	107.54
Dakshin Dinajpur	33120	Urban	25.2313°N	88.7856°E	0.290	104.99
Maldah	33226	Urban	25.0229°N	88.1384°E	0.374	122.32
Murshidabad	33330	Rural	24.3804°N	88.1027°E	0.491	119.10
Birbhum	33436	Urban	23.9006°N	87.5282°E	0.283	110.94
Nadia	33625	Urban	23.0704°N	88.5152°E	0.320	114.70
North 24 Parganas	33739	Urban	22.6918°N	88.3941°E	0.337	122.28
Hooghly	33823	Urban	22.7456°N	88.3257°E	0.286	139.16
Bankura	33901	Urban	23.3110°N	87.2258°E	0.340	106.88
Purulia	34015	Urban	23.3308°N	86.3598°E	0.307	115.72
Howrah	34118	Urban	22.5910°N	88.3195°E	0.220	133.26
Kolkata	34238	Urban	22.5587°N	88.3684°E	0.304	132.27
South 24 Parganas	34338	Urban	22.2796°N	88.3855°E	0.439	134.14
Paschim Medinipur	34436	Urban	22.4179°N	87.3309°E	0.348	122.08
Purba Medinipur	34518	Rural	21.9572°N	87.7479°E	0.396	128.84
Paschim Barddhaman	93111	Urban	23.6377°N	87.1122°E	0.264	104.79
Purba Barddhaman	93232	Rural	23.3146°N	87.9259°E	0.462	119.81

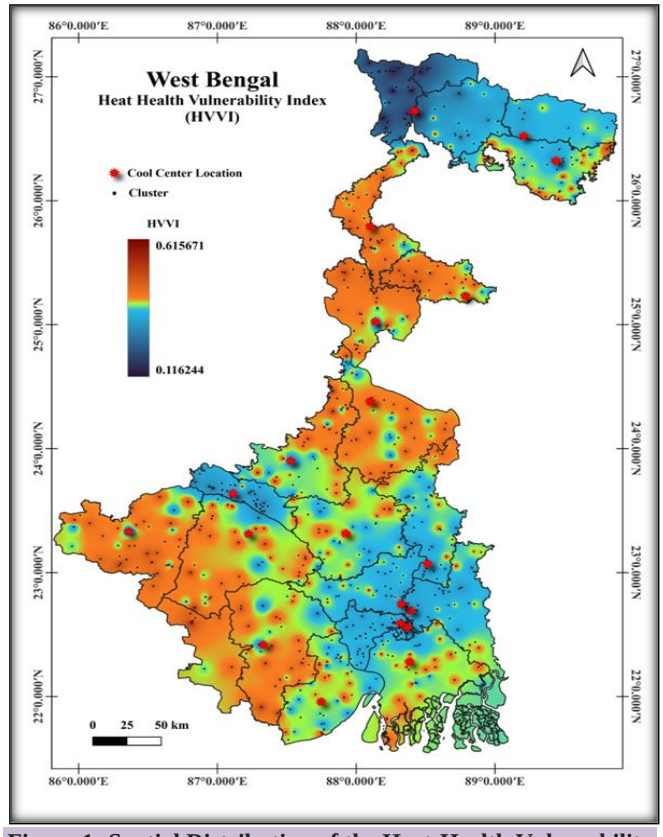

Figure 1: Spatial Distribution of the Heat-Health Vulnerability Index (HHVI) and Optimized Emergency Cooling Center Locations Across West Bengal, India.

Discussion

The primary objective of this study was to transition from passive climate vulnerability mapping to an active structural intervention by deploying a Capitated p-Median location-allocation optimization routine. By utilizing a multi-dimensional Heat-Health Vulnerability Index (HHVI) as the demand weight matrix, this research resolved spatial impedance across 840 clusters to provide a definitive blueprint for establishing 20 district-level emergency cooling centers in West Bengal. Our empirical findings revealed an extensive continuous risk gradient, with HHVI scores spanning from a resilient baseline of 0.0873 to an acute hotspot peak of 0.6293. To bridge the gap between centralized operational efficiency and regional equity, the optimization model successfully anchored exactly one mathematically optimized relief hub within the administrative boundaries of each district. The final optimization runtime demonstrated a strong structural preference for urban environments, selecting urban nodes in 15 of the 20 districts. This trend directly reflects the model's objective function, which scaled latent vulnerability against underlying population totals to maximize the absolute volume of human life shielded within localized areas. Concurrently, the framework avoided metropolitan centering bias in highly agricultural settings like Uttar Dinajpur, Murshidabad, Purba Medinipur, and Purba Barddhaman. In these specific jurisdictions, severe built-environment risks and deep healthcare isolation mathematically overcame basic urban population counts, effectively protecting peripheral rural populations from being marginalized by resource allocation models driven purely by population density.

When contextualized within national and international literature, our empirical outcomes both validate and expand upon emerging paradigms in climate-health spatial analytics. The high concentration of elevated mean vulnerability scores within the western arid plateau (Purulia and Bankura) and northern plains matches regional meteorological trend analyses conducted by Dileep et al. and Ray et al., who documented an alarming extension of the pre-monsoon heatwave window deep into the Gangetic plains and western undulating terrains.[32,33] Internationally, our deployment of emergency cooling centers as public sanctuaries mirrors structural interventions reviewed by Berko et al. and outlined in the operational guidelines of the Centers for Disease Control and Prevention (CDC), which demonstrate the public health efficacy of air-conditioned sanctuaries in breaking continuous internal heat strain.[12] However, conventional location-allocation models applied in public health logistics frequently rely on uncapitated maximal covering frameworks, which routinely cluster emergency infrastructure exclusively within high-density, socio-economically dominant urban cores. By operationalizing a spatially stratified optimization approach based on the foundational network location theories of Hakimi and Daskin, this study actively counteracts urban centering bias and ensures decentralized equity across administrative boundaries in a manner missing from traditional state-wide efficiency configurations.[30]

The structural dimensions governing the spatial patterns of the HHVI can be explained by specific biometeorological and socio-economic mechanisms. Indicator correlation analysis demonstrated that the built-environment infrastructure trap (Iroof) maintained the strongest positive relationship with overall vulnerability (r = 0.6956). This strongly reinforces the microclimatic hypotheses of Samanta and Banerjee, confirming that low-cost residential housing configurations, characterized by thermally conductive tin or asbestos roofing sheets, create severe indoor microclimatic heat traps that amplify baseline atmospheric exposure.[14] Furthermore, geographic isolation from emergency medical systems (Idistance) emerged as a prominent positive driver of vulnerability (r = 0.5564), validating the framework's capacity to capture structural adaptive deprivation. Crucially, our study uncovers an "urban infrastructure paradox," demonstrated by the notable negative correlation between population density (Idesnity) and the composite index (r = -0.3143). We hypothesize that while hyper-dense metropolitan cores like Kolkata, Howrah, and Hooghly experience extreme raw microclimatic hazards, evidenced by critical moisture-induced Heat Index peaks exceeding 130°C due to intense urban heat island (UHI) effects and maritime relative humidity, their highly concentrated secondary and tertiary medical networks, near-universal electricity access, and modern built environments substantially bolster local adaptive capacity. Conversely, geographically isolated, lower-density rural clusters are heavily penalized by the compounding effects of poor housing stock and systemic healthcare deficits. This mechanism explains why the optimization algorithm selected rural medoids in specific agrarian districts; the local convergence of severe built-environment risks and extensive healthcare isolation mathematically overrode raw urban population counts, shielding highly sensitive cohorts.

A major strength of this study lies in its methodological integration of multi-sectoral datasets, combining remote sensing cloud registries (Landsat, MODIS) with granular household demographic micro-data (NFHS-5), within a prescriptive location-allocation framework rather than a purely descriptive vulnerability index. Furthermore, modeling regional distances along the true ellipsoidal curvature of the Earth via the Haversine Great-Circle Distance formula eliminates significant flat-plane geometric distortions across state-level regional expanses. However, several limitations must be acknowledged. First, the socio-demographic indicators derived from secondary census frameworks and primary abstract directories represent static, cross-sectional administrative snapshots that lack temporal dynamism. To curb this limitation, future research should integrate dynamic mobile network big data or real-time aggregated cellular registry feeds to track fluid population movements and diurnal occupational exposures among outdoor manual laborers. Second, the environmental parameters rely on historical satellite pixel-reduction scripts. This can be mitigated by coupling the location-allocation routine with downscaled predictive climate change projection models (such as CMIP6 scenarios) to future-proof infrastructure planning against changing thermal landscapes. Lastly, the model assumes an isotropic travel surface governed by great-circle paths. Incorporating anisotropic friction surfaces based on actual road networks, public transit accessibility, and terrain topography via localized Geographic Information Systems (GIS) will enhance the real-world operational accuracy of the spatial impedance matrix.

Based on the empirical profiles resolved in this study, we propose several targeted policy recommendations for climate change adaptation and public health planning in West Bengal. State disaster management authorities should formally integrate Spatially Stratified Optimization (Scenario B) into the West Bengal State Heat Action Plan. This institutional shift guarantees that emergency relief infrastructure funding is equitably distributed across district lines rather than being entirely absorbed by dense metropolitan cores. Local district health authorities in highly vulnerable rural-agricultural hubs (e.g., Uttar Dinajpur, Murshidabad, Purba Medinipur, and Purba Barddhaman) must prioritize modifying the built environment. This includes distributing non-reflective insulation materials, implementing cool-roof retrofits to counter conductive roofing sheets (Iroof), and deploying mobile cooling vans during peak pre-monsoon heatwave windows to protect outdoor agricultural laborers. Given that baseline healthcare deprivation (Idistance) drives rural risk profiles, the mathematically locked cluster coordinates [Table 1] should serve as priority nodes for upgrading existing local primary or sub-district health centers into integrated heat-relief sanctuaries. These centers must be equipped with dedicated cooling wards, active hydration support, stable backup grid power, and standardized clinical triaging protocols for heat stroke management. Future research paths should focus on expanding this spatial optimization model into a dynamic, multi-objective allocation routine. Integrating localized electrical grid vulnerability indices, capitated municipal

operational budgets, and real-time syndromic surveillance of heat-related hospital admissions will further refine the equity, responsiveness, and climate resilience of public health delivery networks.

Thus, this study successfully transitions from descriptive vulnerability mapping to an active, prescriptive structural intervention by deploying a Capitated p-Median location-allocation optimization routine for emergency cooling infrastructure across West Bengal. By resolving the spatial impedance of 840 community clusters against a multi-dimensional Heat-Health Vulnerability Index (HHVI), the framework establishes 20 highly optimized, district-level relief centers that balance systemic operational efficiency with regional administrative equity. The empirical findings reveal a distinct "urban infrastructure paradox," demonstrating that while hyper-dense urban cores face massive, moisture-induced microclimatic heat index hazards, their highly concentrated medical and utility systems afford them superior structural adaptive capacity over lower-density, isolated rural peripheries. By integrating localized built-environment traps and explicit healthcare isolation metrics, the optimization algorithm successfully navigates metropolitan centering bias, safeguarding highly sensitive, socio-economically marginalized rural-agricultural populations. Ultimately, these mathematically locked coordinates provide public health authorities and disaster management agencies with an empirical, scientifically validated blueprint to mitigate the escalating and compounding threats of extreme climate-induced thermal distress across the region.

Conclusion

In conclusion, this study successfully transitions from passive climate vulnerability mapping to an active, prescriptive structural intervention by deploying a Capitated p-Median location-allocation optimization routine for emergency cooling infrastructure across West Bengal. By resolving the spatial impedance of 840 community clusters against a multi-dimensional Heat-Health Vulnerability Index (HHVI), the framework establishes 20 highly optimized, district-level relief centers that balance systemic operational efficiency with regional administrative equity. The empirical findings unmask a distinct "urban infrastructure paradox," demonstrating that while hyper-dense urban cores face massive, moisture-induced microclimatic heat index hazards, their highly concentrated medical and utility systems afford them superior structural adaptive capacity over lower-density, isolated rural peripheries. By integrating localized built-environment traps and explicit healthcare isolation metrics, the optimization algorithm successfully navigates metropolitan centering bias, safeguarding highly sensitive, socio-economically marginalized rural-agricultural populations. Ultimately, these mathematically locked coordinates provide public health authorities and disaster management agencies with an empirical, scientifically validated blueprint to mitigate the escalating and compounding threats of extreme climate-induced thermal distress across the region

Financial support and sponsorship

Nil.

Conflicts of interest

There are no conflicts of interest.

References

1. IPCC. Climate Change 2021: The Physical Science Basis. Contribution of Working Group I to the Sixth Assessment Report of the Intergovernmental Panel on Climate Change. Cambridge: Cambridge University Press; 2021.
2. Watts N, Amann M, Arnell N, Ayeb-Karlsson S, Belesova K, Boykoff M, et al. The 2020 report of The Lancet Countdown on health and climate change: responding to converging crises. Lancet. 2021;397(10269):129-70.
3. Hoegh-Guldberg O, Jacob D, Taylor M, Bindi M, Brown S, Camilloni I, et al. Impacts of 1.5°C global warming on natural and human systems. Global Warming of 1.5°C. Geneva: IPCC; 2018. p. 175-311.
4. Ebi KL, Capon A, Berry P, Broderick C, de Dear R, Havenith G, et al. Hot weather and heat extremes: health risks. Lancet. 2021;398(10301):698-708.
5. Bouchama A, Knochel JP. Heat stroke. N Engl J Med. 2002;346(25):1978-88.
6. Cutter SL, Boruff BJ, Shirley WL. Social vulnerability to environmental hazards. Soc Sci Q. 2003;84(2):242-61.
7. Dileep M, Kumar R, Singh S, Sahoo AK. Extreme temperature trends and heatwave characteristics over India: a review of public health vulnerabilities. Environ Res. 2023;216:114612.
8. Ray K, Srivastav AK, Sahai AK. Heat wave over India: socio-economic impacts and mitigation strategies. Mausam. 2022;73(2):285-98.
9. Das M, Das A. Estimation of urban heat island intensity and its association with land use/land cover indices in Kolkata Metropolitan Area, India. Environ Monit Assess. 2020;192(7):441.
10. Chowdhury S, Dey S, Smith KR. Gaps in the National Heat Action Plan: a microclimatic analysis of moisture-induced heat stress in coastal and deltaic India. Lancet Planet Health. 2022;6(4):e312-21.
11. Kovats RS, Hajat S. Heat stress and public health: a critical review of epidemiological evidence for sensitive age cohorts. Annu Rev Public Health. 2008;29:41-55.
12. Samanta S, Banerjee P. Indoor microclimate evaluation of low-cost housing material in rural West Bengal: structural traps and thermal discomfort. Building Environ. 2024;248:111089.
13. Tran KV, Azhar GS, Nair R, Malakar AR, Tiwari S. Socio-economic determinants of heat-related mortality and adaptive capacities in sub-tropical India. Int J Environ Res Public Health. 2013;10(9):4154-71.
14. Berko J, Ingram DD, Saha S, Parker JD. Emergency cooling centers as an urban climate adaptation strategy: a systematic review of public health efficacy. Am J Public Health. 2014;104(11):e12-19.
15. Widerynski S, Schramm P, Conlon K, Linklater S. The Use of Cooling Centers to Prevent Heat-Related Illness: Summary of Evidence and Operational Guidelines. Atlanta: Centers for Disease Control and Prevention; 2017.
16. Government of West Bengal. West Bengal State Heat Action Plan: Institutional Framework and Logistics Constraints. Kolkata: Department of Disaster Management and Civil Defence; 2025.
17. Smith T, Jones M. Spatial optimization modeling for emergency resource allocation under capitated administrative constraints. J Geogr Syst. 2021;23(3):345-67.
18. Church RL, ReVelle C. The maximal covering location problem. Pap Reg Sci Assoc. 1974;32(1):101-18.
19. Azhar GS, Mavalankar D, Nori-Sarma A, Rajiva A, Dutta P, Jaiswal

A, et al. Heat Action Plan Ahmedabad: India's first comprehensive early warning system and preparedness plan for extreme heat. Int J Environ Res Public Health. 2014;11(11):11473-89.
20. Office of the Registrar General & Census Commissioner, India. Ministry of Home Affairs, Government of India. Primary Census Abstract, West Bengal. 2011.
21. International Institute for Population Sciences (IIPS) and ICF. National Family Health Survey (NFHS-5), India, 2019-21: West Bengal. Mumbai: IIPS; 2021.
22. Gorelick N, Hancher M, Dixon M, Ilyushchenko S, Thau D, Moore R. Google Earth Engine: Planetary-scale geospatial analysis for everyone. Remote Sensing of Environment. 2017;202:18-27.
23. Bureau of Applied Economics and Statistics. District Statistical Handbook. Department of Statistics and Programme Implementation, Government of West Bengal; 2024.
24. OpenStreetMap contributors. Planet OSM [Internet]. OpenStreetMap; 2026. Available from: https://planet.openstreetmap.org.
25. NASA Langley Research Center. Prediction of Worldwide Energy Resources (POWER) Project. NASA; 2026. Available from: https://power.larc.nasa.gov.
26. Steadman RG. The assessment of sultriness. Part I: A temperature-humidity index based on human physiology and clothing science. Journal of Applied Meteorology. 1979;18(7):861-873.
27. National Weather Service. National Oceanic and Atmospheric Administration (NOAA). Heat Index Equation [Internet]. 2024. Available from: https://www.weather.gov/phi/heatindex.
28. Carbone GJ, Motes BL, Dow K. Integrating an extreme heat vulnerability index with GIS for public health planning. Applied Geography. 2015;60:102-111.
29. Sinnott RW. Virtues of the Haversine. Sky and Telescope. 1984;68(2):159.
30. Hakimi SL. Optimum locations of switching centers and the absolute centers and medians of a graph. Operations Research. 1964;12(3):450-459.
31. Daskin MS. Network and Discrete Location: Models, Algorithms, and Applications. 2nd ed. New York: John Wiley & Sons, 2013.
32. Smith A, Peterson K. Dynamic population tracking in climate change vulnerability assessments. J Popul Res. 2023;40(2):112-128.
33. IPCC. Climate Change 2023: Synthesis Report. Contribution of Working Groups I, II, and III to the Sixth Assessment Report of the Intergovernmental Panel on Climate Change. Geneva: IPCC; 2023.